CH30132

Exploratory Synthesis of Sodalite with Altered Fluorescence

Michael Kubiak

20978

Supervisor: ***Professor Mark Weller***

Plagiarism Declaration

I certify that I have read and understood the entry in the Student Handbook for the Department of Chemistry on Cheating and Plagiarism and that all material in this assignment is my own work, except where I have indicated with appropriate references.

I agree that, in line with Regulation 15.3(e), if requested I will submit an electronic copy of this work for submission to a Plagiarism Detection Service for quality assurance purposes.

Student Name: Michael Kubiak

Date: 10th July 2018

Abstract

The fluorescent properties of sodalite were investigated. The intense yellow-orange fluorescence of sodalite is due to $[S_2]^-$ ions. Other fluorescence colours are seen due to differences in composition or synthesis. In this work, blue fluorescence was investigated by altering the synthesis process of sodalites, with the formula $Na_8(AlSiO_4)_6(Cl,S)_2$, to discover which factors affected the appearance of blue fluorescence. Once this had been determined, the synthesis was optimised to provide the most intense blue fluorescence. Measurements were made to determine the structure, composition and the properties of samples of synthetic sodalite and explore their relationship. Samples were synthesised that had a high intensity of blue fluorescence compared to the maximum intensity of orange fluorescence that had been achieved. Some progress was made towards determining the cause of the blue fluorescence.

Contents

1 Introduction

1.1 Photo-luminescence and Tenebrescence

Luminescence refers to a light emitted, at room temperature or lower, by an electron returning from an excited state to a lower energy state following its excitation by an energy source, [The Fluorescent Mineral Society, 2013].

Photo-luminescence is luminescence caused by the absorption of light. There are two forms of photo-luminescence, illustrated in figure 1. The first is fluorescence, where a photon excites an electron, which loses some energy by non radiative transitions, then radiates a lower energy photon as it returns to a lower energy level. The second photo-luminescence property, phosphorescence occurs when the electron moves (again by non radiative processes) into a longer lived state, rather than fluorescing. As this state is somewhat stable, the molecule remains in the state, and the material radiates over a much longer time period.

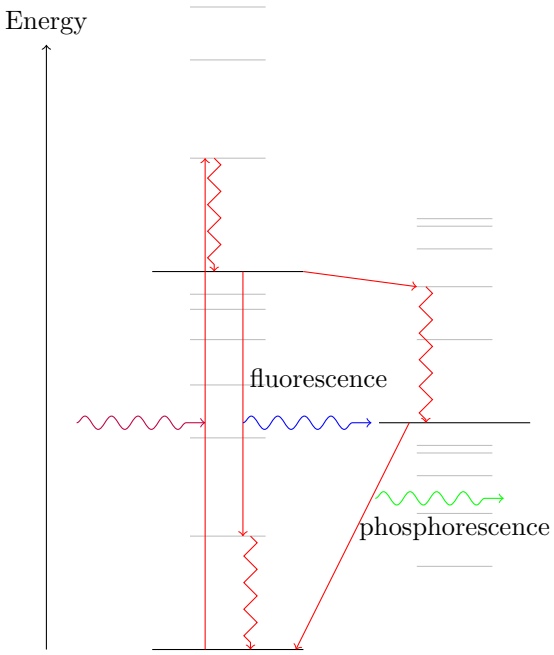

Figure 1: A simple diagram to explain photo-luminescence properties. Electronic energy levels are black lines, vibrational energy levels are grey lines, energy change is shown in red and other arrows are photons

Tenebrescence is a type of reversible photochromism seen in minerals. Photochromism is a property where absorbing a particular wavelength of light causes a molecule to change its properties or structure such that its colour changes. Tenebrescence is demonstrated in figure 2.

1.2 Current Fluorescent Materials

Fluorescent materials are mainly used as phosphors in LCDs and white LEDs. Most fluorescent materials currently in use contain rare earth element ions. Examples include $BaMgAl_{10}O_{17}:Eu^{2+}$ (figure 3a), which is discussed in [Kim et al., 2002], and $Y_2O_3:Eu^{3+}$ (figure 3b), discussed in [Song et al., 2002]. The electronic transitions of the rare earth ions are the cause of the fluorescence seen. To produce white light, a mixture of colours are required. This normally requires either a yellow phosphor that absorbs blue light, so that a

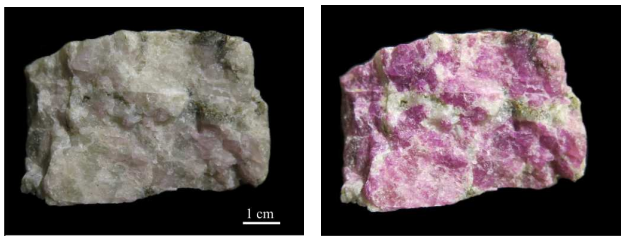

(a) (b)

Figure 2: Pictures showing a tenebrescent sample a) before irradiation, and b) after irradiation with UV, from the supporting material for [Zahoransky et al., 2016]

blue emitting LED can be used, or a mixture of red, green and blue phosphors. Rare earth elements are expensive, as they are environmentally unfriendly to mine, and difficult to extract from ores. Due to these problems with rare earth elements, different types of phosphors are being investigated. One family of alternative phosphor is based on the naturally occurring mineral sodalite. These can be relatively cheaply synthesised from commonly used, and easily synthesised, precursors, see [Dreyfus and Hornberger, 1971], and so would be much less expensive and more environmentally friendly to produce than the currently used phosphors.

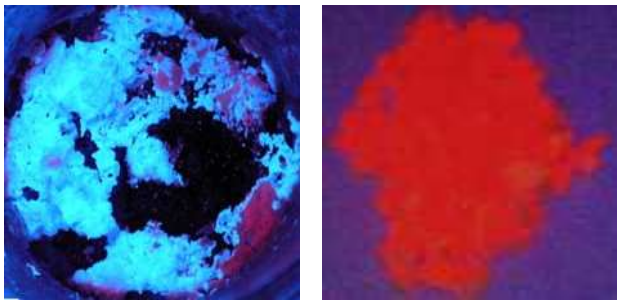

(a) (b)

Figure 3: a) is $BaMgAl_{10}O_{17}:Eu^{2+}$ fluorescence from [Pradal et al., 2011] b) is $Y_2O_3:Eu^{3+}$ fluorescence from [Wang et al., 2012]

1.3 Sodalite

The sodalite structure is shown in figure 4a. Sodalites are formed from cages made of aluminium and silicon, linked by oxygen, inside which anions and cations reside. In the case of the structure shown below, where the anions are chloride and the cations are sodium, the formula of the sodalite is $Na_8(Al_6Si_6O_{24})Cl_2$ and, when it is pure, it has no optical properties in the visible part of the spectrum. Natural sodalites, from Greenland and Canada, such as that seen in figure 4b, on the other hand, tend to be coloured, or have luminescent, as is visible in figure 4c, and tenebrescent properties when exposed to light in the UV part of the spectrum.

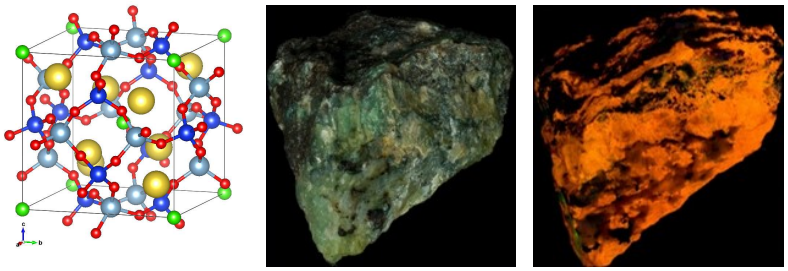

(a) (b) (c)

Figure 4: a) Sodalite structure drawn from [Pauling, 1930], with silicon shown in blue, aluminium in silver, sodium in yellow, chloride in green, and oxygen in red, b) natural sodalite from Greenland and c) a piece of fluorescent sodalite under a 365 nm lamp

1.3.1 Fluorescence in Sodalite

Fluorescent properties of sodalites have been discussed in many publications since its discovery, from [Kirk, 1955], to [Norrbo et al., 2016]. The orange fluorescence, figure 4c, that is usually seen, and the tenebrescence, are thought to be connected to the sulfur content of the sodalite, [Kirk, 1955]. [Kirk et al., 1965], confirmed that this orange fluorescence required the $[S_2]^-$ ion. Other colours of fluorescence have also been seen in sodalite, and many different ions found within the structure have been postulated as possibly having a role in some of the luminescent properties that have been seen. This includes Mn^{2+}, for red fluorescence, and Fe^{3+}, for green fluorescence, [Kaiheriman et al., 2014].

It has been discovered that the orange fluorescence in sodalite can be shifted by exchanging the cations within the sodalite for Ag^{+}, Cd^{2+} and Pb^{2+}, [Mikuła et al., 2016]. Preliminary work was performed on Ag^{+} ion exchange, as well as experiments in Li^{+} and Fe^{2+} ion exchange but this investigation was still at an early stage, and will not be presented further.

1.3.2 Blue Fluorescence

As well as those luminescences mentioned above, sodalite can also show a blue fluorescence, that has not been completely studied yet. A recent paper, [Norrbo et al., 2016], ascribes the blue fluorescence to a Ti impurity within the sodalite structure. An emission spectrum from the sample produced in this paper is shown in figure 5.

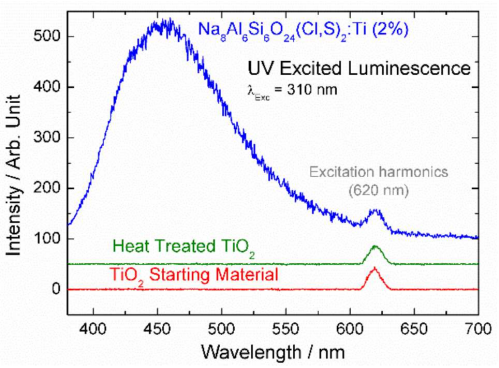

Figure 5: Blue fluorescence spectrum from doped sodalite, from [Norrbo et al., 2016]

1.3.3 Aims

The experiments reported here aimed to optimise the intensity of blue fluorescence produced by sodalites, synthesised by a solid state route, without the addition of extra Ti. This was done by looking for the best synthesis procedure to produce a brightly luminescent sample. The structural and compositional differences between samples of sodalite with the different fluorescence colours and intensities were also investigated.

2 Experimental

The synthesis of sodalite with orange fluorescence had been optimised by a member of the group among which this project was performed, and the work leading to it is, as yet, unpublished. This method was the starting point for the exploration of blue fluorescence in sodalite reported here, as it provided the optimal salt ratio and temperature for the appearance of the most intense orange fluorescence.

2.1 Synthesis

Sodalite samples were synthesised by a solid state route with a fixed optimised salt ratio (for the most intense orange fluorescence) to ensure that a sodalite with the most intense blue fluorescence possible was obtained. This salt ratio had also been found to form a single phased sodalite, which was not the case for higher ratios of sulfur. The combined molar quantity of NaCl (Sigma-Aldrich, $\geq$99.8 %) (182 mg, 3.11 mmol) and Na_2SO_4 (Fisher Scientific, analytical reagent grade) (221 mg, 1.56 mmol) were in large excess of the possible molar quantities of the fixed mass of zeolite 4A (Sigma-Aldrich, product 23,366-8) (600 mg), based on its varying molar mass, which changes with humidity. This was done to ensure that no unreacted zeolite would remain in the product of the reaction, and also to form the most thermodynamically stable sodalite for reproducibility. This precursor mixture was ground together, then heated in a quartz crucible using a tube furnace, shown in figure 6, to 250 °C under a flow of H_2 for 3 h to dehydrate the zeolite. It was then heated for a further 20 h under H_2. This further heating occurred at different temperatures for different samples. These were 650 °C, 600 °C and 575 °C. A scheme for the synthesis is shown in figure 7.

Once the product had cooled, it was separated into 200 mg parts. An oxidation step was performed on some of the parts by heating them to 850 °C for between 5 min and 20 min under air. These different oxidations steps were investigated for many of the samples, but it was found that the best samples to use

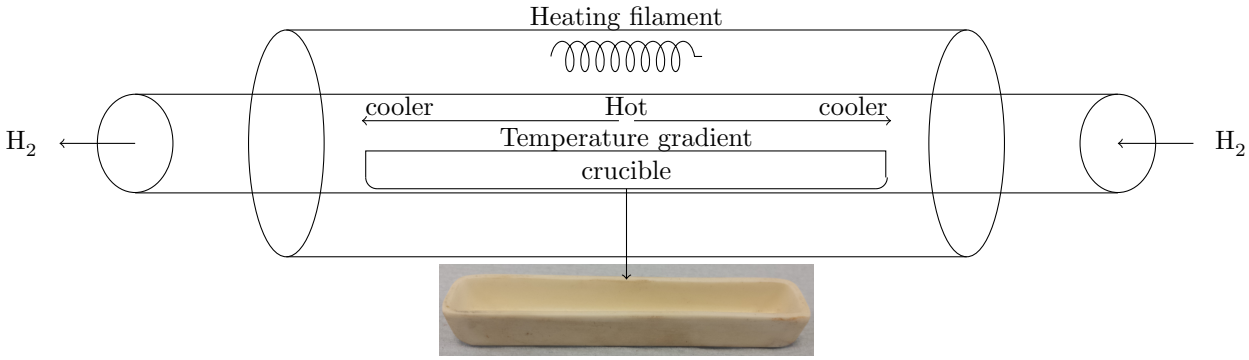

Figure 6: Synthesis furnace set-up

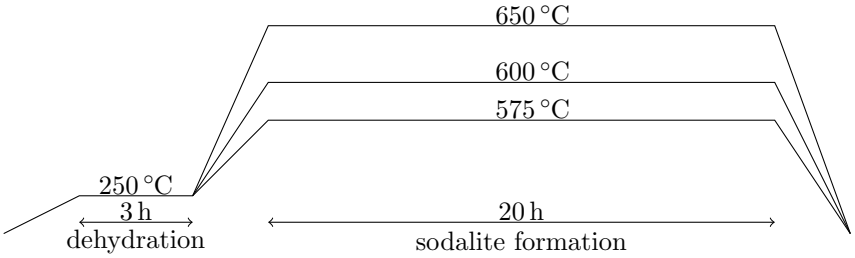

Figure 7: Synthesis scheme for sodalites

for comparison were those which had not been oxidised (+0), which showed the most intense blue fluorescence, and those which had been oxidised for 15 min (+15), which showed the most intense orange fluorescence. The others showed less fluorescence, and so were not investigated further.

The samples were washed with distilled water to remove excess salt before characterisation.

Samples will be referred to by their colours of fluorescence followed by their synthesis temperature. A table of all relevant experiments performed, along with their names, is shown in figure 8.

2.2 Characterisation

- Powder X-Ray Diffraction (PXRD) patterns were taken using a Bruker D8 Advance instrument using $Cu_{K\alpha}$ (λ= 1.540 598 Å) X-ray radiation and a Lynx-Eye detector. Le Bail and Rietveld refinements (see Appendix B) of the structure were performed using JANA 2006. The pattern of a chloride sodalite was used for all refinements, because sulfur and chloride can not be differentiated by XRD.
- Energy Dispersive X-ray spectroscopy (EDX) was performed in a scanning electron microscope (JEOL SEM6480LV) chamber. Spectra were obtained at 10 kV under low vacuum using backscattered electron imaging and an Oxford INCA X-Act SDD X-ray detector.
- Infra-Red (IR) spectra were taken by a Perking Elmer Frontier FTIR spectrometer with a diamond ATR head. They were taken between 4000 cm^{-1} and 600 cm^{-1} with an improved resolution MCT detector.
- Fluorescence spectra were taken using a Perkin Elmer LS55 Luminescence Spectrometer with a R928 photomultiplier and a Xenon discharge lamp. All fluorescence spectra that had comparisons drawn between them were taken with the same set-up of the spectrometer.

Synthesis Temperature (°C)	Oxidation Step (min)	Fluorescence Colour	Number of Samples Produced	Name
650	0	None	2	OF650
	5	Orange	2	
	15	Orange	2	
	20	Orange	2	
	0	Blue	1	OBF650
	5	Orange	1	
	15	Orange	2	
	20	Orange	1	
600	0	Blue	1	BF600
	5	None	1	
	15	None	1	
575	0	Blue	1	BF575
	5	None	1	
575 + 5 h	0	Blue	1	BF575 +5 h
575 (Cl only)	0	None	1	NF575

Figure 8: Table of relevant experiments performed

3 Results and Discussion

3.1 Structure and Composition

Three techniques were used to determine structure and composition. PXRD allowed discovery of what phases were present in a sample, and how they related to known structures. It could also used be to discover the positions of atoms. EDX was used to discover the composition of the samples. IR shows the vibration of bonds, and so allows the linkage between atoms to be probed. IR is often used together with XRD, as they tend to provide different structural information.

3.1.1 XRD

Figure 9 shows a comparison of XRD patterns for each of the samples with blue fluorescence with the pattern for the sample with orange fluorescence. It can be seen that the lower temperature syntheses produce less pure samples, as the samples synthesised at 650 °C have almost identical patterns, while the 600 °C and 575 °C spectra have extra peaks, which increase in size with lower temperature.

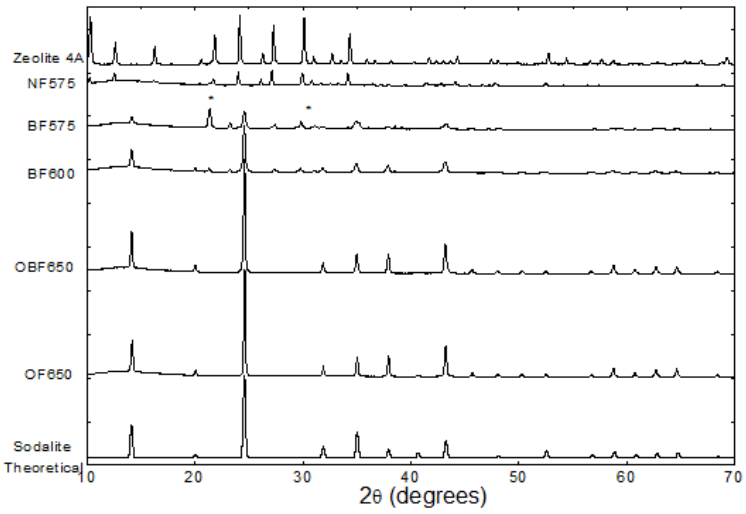

Figure 9: Comparison of XRD patterns of OF650, OBF650, BF600, BF575 and NF575. Asterisks show nepheline peaks.

Figure 10 shows the Rietveld refinement which fits the pattern of a chloride sodalite, shown above the pattern, to that of OF650. This demonstrates that this sample only contains sodalite with a somewhat larger lattice parameter compared to the chloride sodalite (8.896024 compared to 8.87). This difference in lattice parameter may be due to the larger $[S_2]^-$ ions.

The Le Bail refinement to fit the XRD pattern of BF600 is shown in figure 11. It can be seen that there is an extra phase in this sample, nepheline, whose structure is shown above the pattern.

Figure 12 shows the Le Bail refinement to fit the XRD pattern of BF575 to patterns of zeolite, nepheline and a chloride sodalite. There are a number of peaks which correspond to zeolite, which implies that 575 °C is not a high enough temperature to get a complete reaction. There is also more nepheline compared to the amount of sodalite in this sample, which suggests that nepheline forms at a lower temperature than sodalite.

Figure 13 shows the Le Bail refinement to fit the XRD pattern of a sample with no sulfur, NF575. No Rietveld refinement could be performed, as there were too many phases. It is obvious that there was a small amount of sodalite and some nepheline, but the majority remained as zeolite.

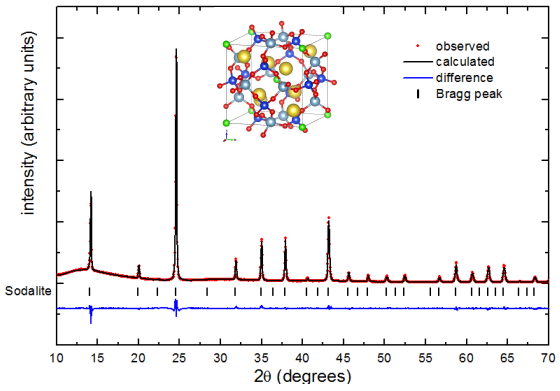

Figure 10: Rietveld refinement to fit the pattern of a chloride sodalite (shown above the pattern) to the experimentally observed XRD pattern of OF650

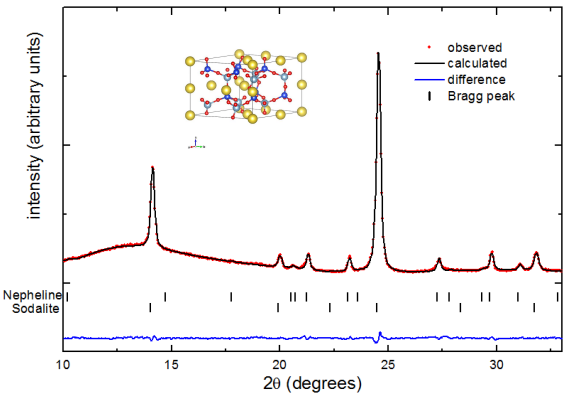

Figure 11: Le Bail refinement to fit the patterns of a chloride sodalite and nepheline (shown above the pattern) to the experimentally observed XRD pattern of BF600

Summary

XRD shows that the product of the synthesis was affected greatly by the temperature at which the synthesis took place. A synthesis temperature of 650 °C produced a single phase, which refined well to a sodalite with a slightly larger lattice parameter than the pattern (8.896024 compared to 8.87), which contained no sulfur anions. This difference might be due to the presence of the sulfur. Lower temperature syntheses produced a different aluminosilicate phase, nepheline, and caused some zeolite to remain unreacted.

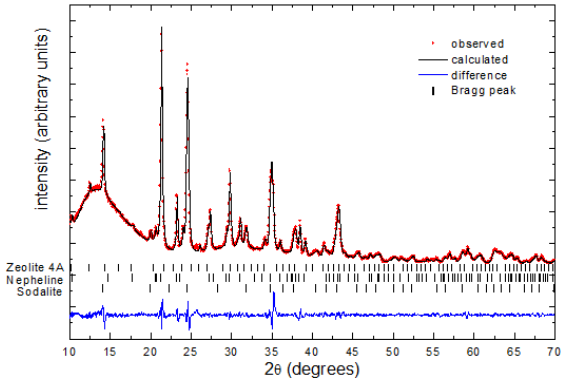

Figure 12: Le Bail refinement fitting the XRD pattern of BF575 to the patterns of zeolite 4A, nepheline and a chloride sodalite

3.1.2 Elemental Analysis

The sodalites were expected to have a formula of $Na_8(AlSiO_4)_6(Cl_{2-2x-\delta}S_\delta(SO_4)_x)_2$. EDX cannot differentiate S from SO_4, and XRD showed that there were multiple phases, so the formula of the sodalite in the samples could not be determined from EDX. The ratio of aluminium to silicon, and the percentage of sulfur in each sample are shown in figure 14. The Al/Si ratio is relatively constant through all of the samples, and shows a higher silicon content than the expected formula. The percentage of sulfur appeared to be much greater in BF600 than in any of the other samples. This could be due to an incomplete washing of the sample, or the lower temperature may have caused a sulfur sodalite to form more preferentially. The fact that BF575 had a much smaller percentage of sulfur may be accounted for by the other aluminosilicates in the sample, which do not require anions, and so would decrease the overall percentage of sulfur, even if the sodalite that did form contained more sulfur.

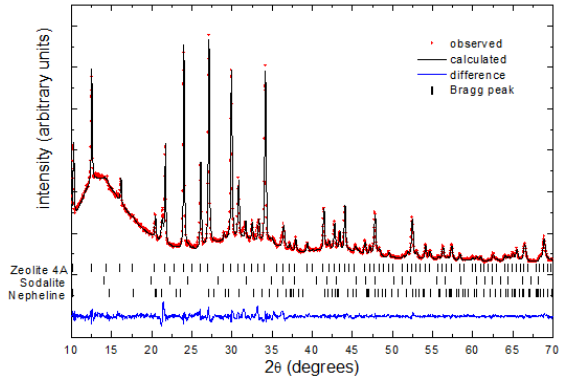

Figure 13: Le Bail refinement fitting the XRD pattern of NF575 to the patterns of zeolite, nepheline, and a chloride sodalite

Sample	Al/Si	%S
OF650	0.92(2)	24(2)
OBF650	0.85(2)	25.3(9)
BF600	0.87(4)	39(3)
BF575	0.89(2)	12(1)
NF575	0.84(2)	-

Figure 14: A table of the mean ratio of aluminium and silicon, and of the percentage sulfur content of each sample from a variety of measurements at multiple sites on the material

3.1.3 IR Spectroscopy

The IR spectra of the samples with blue fluorescence compared to the sample with orange fluorescence and the zeolite used in the synthesis of the samples are shown in figure 15. No relevant peaks were seen at higher wavenumbers than 1200. The main difference between the spectra is seen in the peaks between 550 cm^{-1} and 650 cm^{-1}. There appears to be a peak, not visible in the spectrum of the samples synthesised at 650 °C, that increases in height for lower temperature synthesis. This peak is likely to be due to the Si-O-Al bonds in the nepheline structure, which was seen in XRD, as it is not accounted for by the precursor, Zeolite 4A.

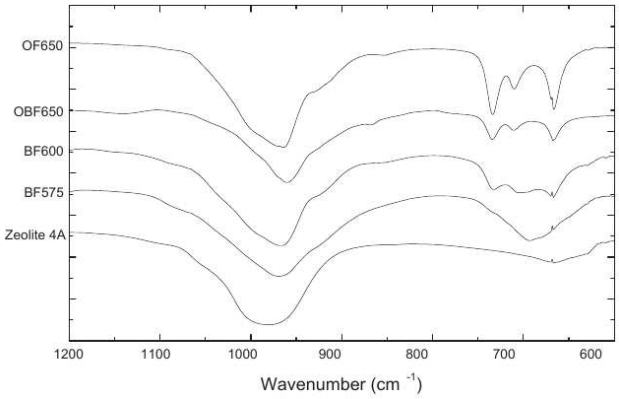

Figure 15: Comparison of normalised IR spectra of OF650, OBF650, BF600, BF575 and zeolite 4A

3.2 Fluorescence Measurements

T = 650 °C

The fluorescence spectra of OF650 are shown in figures 16 and 17 for comparison. The peaks seen in figure 16 (+15) between 500 nm and 750 nm in the 365 nm emission spectrum and between 300 nm and 500 nm in the 615 nm excitation spectrum show orange fluorescence. Figure 17 (+0) has a small peak between 250 nm and 500 nm in the 254 nm emission spectrum, which shows a blue fluorescence. The +15 plot shows shows that this blue peak reduced after an oxidation step. Blue fluorescence was not detectable under a lamp at 254 nm excitation.

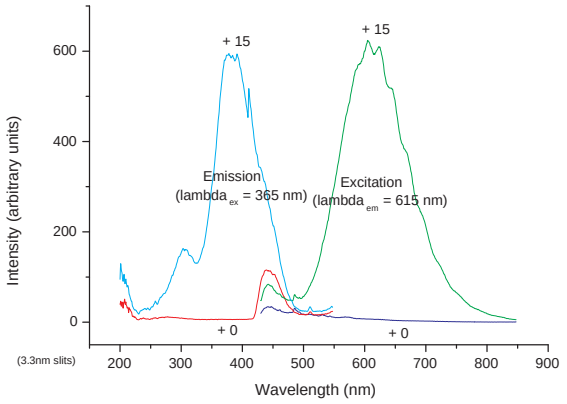

Figure 16: Emission spectra, under 365 nm excitation, and excitation spectra, with 615 nm emission, of OF650 +0 and +15

Figures 18 and 19 show fluorescence spectra for OBF650. The blue fluorescence seen in 19 (+0) was detectable under a UV lamp at 254 nm excitation. Figure 18 (+15) shows roughly the same wavelength of orange fluorescence that was present in figure 16, but, in figure 19 (+15), as in the equivalent for OF650, the intensity of the blue fluorescence decreased greatly after an oxidation step. This demonstrates that the oxidation step, which is necessary for the orange fluorescence to occur, prevents the blue fluorescence from occurring. The difference between the spectra of OF650 and OBF650 are thought to have occurred due to the temperature gradient within the tube furnace shown in figure 6.

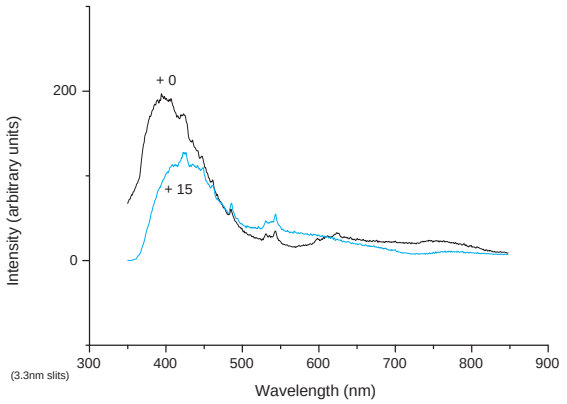

Figure 17: Spectra under 254 nm excitation of OF650 +0 and +15

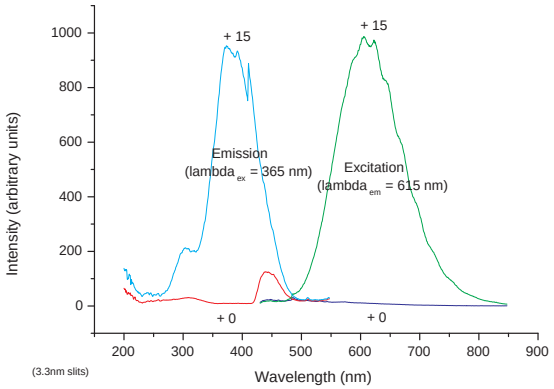

Figure 18: Emission spectra, under 365 nm excitation, and excitation spectra, with 615 nm emission, of OBF650, +0 and +15

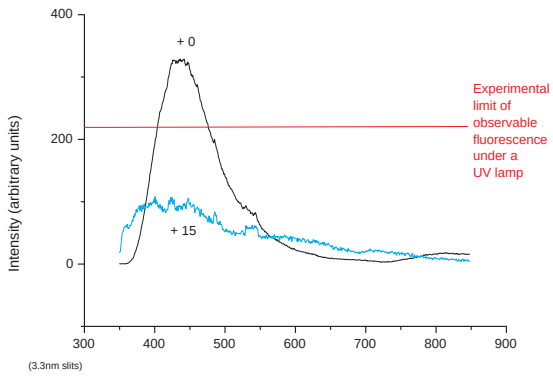

Figure 19: Spectra under 254 nm excitation of OBF650 +0 and +15

T = 600 °C

The fluorescence spectra for BF600 are shown in figures 20 and 21. Figure 20 shows that there was a much lower intensity of orange fluorescence after a 15 min oxidation step than there had been in OF650 and OBF650. This implies a difference in the amount of the species that produces orange fluorescence. Figure 21 shows that this sample had a more intense blue emission than OBF650, which confirmed that the blue fluorescence was related to temperature of synthesis.

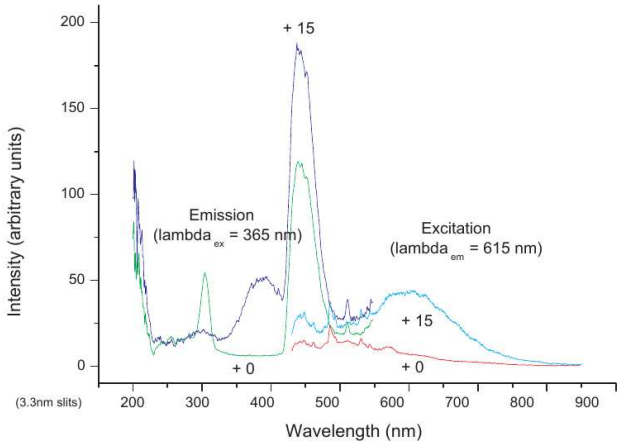

Figure 20: Emission spectra, under 365 nm excitation, and excitation spectra, with 615 nm emission, of BF600 +0 and +15

T = 575 °C

There was no orange fluorescence in BF575, so the spectra have been omitted from further discussion. Also, the effect of the oxidation step on temperature has been demonstrated by the previous samples, so investigation of this was not performed for further samples. The emission spectrum, under 254 nm excitation, for BF575 +0 is shown in figure 22 and shows a reduced peak size compared to BF600, suggesting that less of the cause of the blue fluorescence was present after synthesis at this temperature.

It had previously been found that regrinding and an extra heating, under H_2 at the same temperature, improved orange fluorescence intensity in synthetic sodalites, because it homogenised the sample, allowing for a more even reaction. On cooling after synthesis, half of BF575 had a less intense blue fluorescence due to the temperature

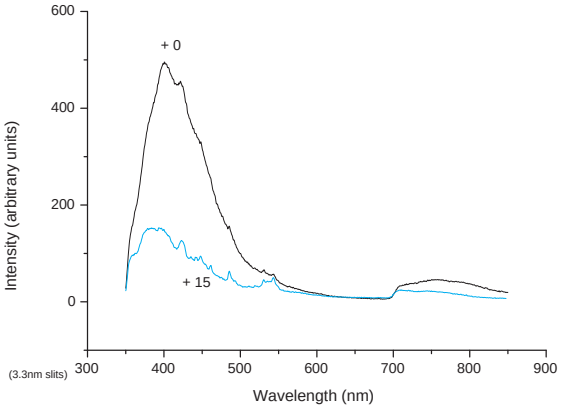

Figure 21: Spectra under 254 nm excitation of BF600 +0 and +15

gradient in the furnace (see figure 6) and a slightly shifted placement of the crucible, so this half was reground and heated to 575 °C for a further 5 h under H_2 for the same purpose, and will be called +5 h. The fluorescence spectrum for this is shown in figure 23. The detector saturated when attempting to take the emission spectrum at 254 nm, so the set-up of the fluorimeter was changed to prevent this. This reduced the intensity of the measured peak. The fluorimeter was set up to be able to record the most intense emission from the orange samples that had been studied previously, which meant that the blue fluorescence from this sample when excited at 254 nm was more intense than the most intense orange fluorescence that had previously been produced.

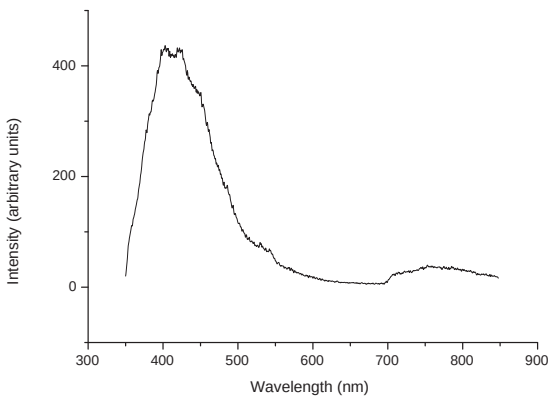

Figure 22: Spectrum under 254 nm excitation of BF575 +0

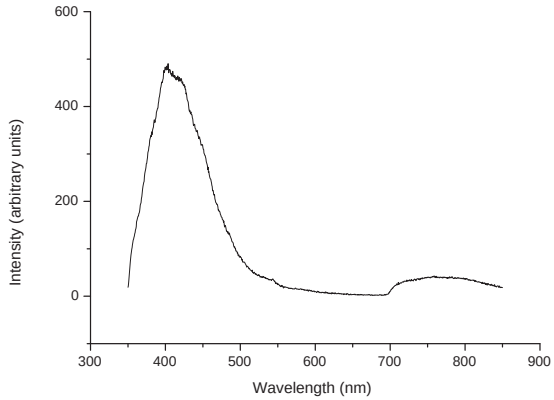

Figure 23: Spectrum under 254 nm excitation of BF575 +5 h. This spectrum is not comparable with the +0 spectrum

No fluorescence was expected in NF575 if the S was involved in causing blue fluorescence within the other samples. This was found to be the case.

Temperature Comparison

Figure 24 compares the emission spectra of the samples with blue fluorescence. It can be seen that OBF650 has the lowest intensity, followed by BF600, then BF575 +5 h. BF575 +5 h has fluorescence with 2 - 3 times the intensity of the fluorescence of BF600, where before the homogenisation and reheating, it was slightly less intense (figures 21 and 22). This shows that the homogenisation and reheating improved the fluorescence to a large degree.

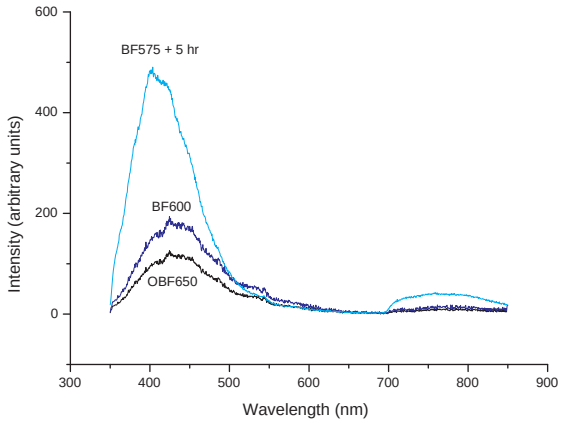

Figure 24: A comparison of emission spectra under 254 nm excitation from samples with blue fluorescence synthesised at different temperatures

Time Dependence of Fluorescence

Figure 25 demonstrates the effect of time under 302 nm radiation on fluorescence of BF600. A total of 20 spectra were taken consecutively, with each spectrum being 67 s long. The main plot shows the first and final spectra, and it can be seen that the intensity reduced. This reduction appears to fit an exponential decay, as shown to the right in a plot of maximum intensity of the fluorescence spectrum against time. This model implies a fast decay to just under two thirds of the maximum intensity of emission, then a relatively stable fluorescence. This decay could be due to tenebrescence, as it occurs due to the same stimulus.

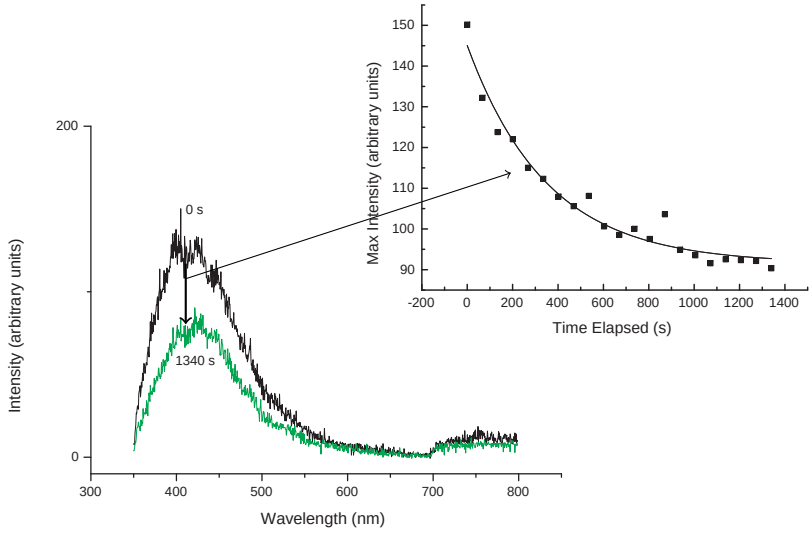

Figure 25: The relation between peak intensity and time under 302 nm radiation is shown. The emission spectra, under 302 nm excitation, of BF600 before and after an extended period of exposure to 302 nm UV radiation are shown. The peak heights for 20 consecutive emission spectra, under 302 nm excitation, of BF600 are fitted to an exponential decay

Summary

Fluorescence spectra show that the intensity of blue fluorescence is improved by a lower synthesis temperature, but if the synthesis temperature is too low, the intensity decreases again. This is due to a decrease in formation of products during the synthesis, as shown in the XRD section. Blue fluorescence intensity is also increased by a homogenisation and reheating step. The spectra show that blue fluorescence is inhibited by the oxidation step which is used to cause synthetic sodalites to exhibit orange fluorescence.

Blue fluorescence intensity is shown to decrease on extended exposure to 302 nm light. This decrease follows an exponential decay curve towards some non-zero value.

4 Conclusions and Future Work

Samples of sodalite with a blue fluorescence were synthesised at three different temperatures (650 °C, 600 °C and 575 °C) to discover the temperature dependence of intensity of blue fluorescence for sodalite.

XRD shows that the lower temperature samples did not form pure sodalite, with nepheline being formed as a side product, as well as some zeolite remaining unreacted. It is not known whether the blue fluorescence may have been due to the nepheline rather than the sodalite, and so an experiment using a synthesis method that produces purer nepheline should be performed in the future.

EDX showed that all of the samples had similar proportions of silicon compared to aluminium, which was expected because the phases found by XRD all had formulae with the same silicon to aluminium ratio. The percentage of sulfur within the samples was seen to increase by a large amount for a 600 °C synthesis, and decrease again for a 575 °C synthesis. The high sulfur content of BF600 could have been due to incomplete washing, so the edx should be repeated with a washed sample to confirm whether this is the case. Otherwise, it is possible that the lower temperature synthesis causes sulfur sodalite to be produced preferentially, but the 575 °C had too much of the other phases, nepheline and zeolite 4A, which masked the increase in sulfur peak.

IR showed growth of one peak, which was shown not to be related to either sodalite or zeolite 4A, with reduced synthesis temperature. This peak was likely to be due to vibrations in the Si-Al bonds in nepheline, the other structure seen in XRD.

There was found to be a great temperature dependence of blue fluorescence, with the greatest intensity of blue fluorescence from a sample that had not been enhanced by further steps at 600 °C. It was also found that the intensity of blue fluorescence of a sample synthesised at a temperature lower than the temperature which gave a maximum intensity could be increased by a further heat treatment at the same temperature. Future work should include an investigation of temperatures between those investigated here, to determine the synthesis method which would provide the maximum intensity of blue fluorescence from a sample made in this way. There should also be an investigation into how salt ratio effects blue fluorescence in sodalite, as the salt ratio used was chosen as it provided the most intense orange fluorescence, but this does not necessarily hold true for the blue fluorescence.

Experiments into the post synthesis homogenisation and reheating should also be performed, as this provided a large increase in blue fluorescence intensity for the sample which underwent it, but it cannot be determined whether this was due to an incomplete reaction being continued, or another mechanism which might improve the higher temperature samples as well. It should also be investigated whether the time for which the sample is reheated has an effect on the increase of fluorescence seen.

References

R. W. Dreyfus and W. P. Hornberger. Synthesis of Photochromic Sodalite by a Diffusion Process. Patent: US154651, 1971.

M. Kaiheriman, A. Maimaitinaisier, A. Rehiman, and S. Aierken. Photoluminescence properties of green and red luminescence from natural and heat-treated sodalite. *Physics and Chemistry of Minerals*, 41(3): 227–235, 2014.

K.-B. Kim, Y.-I. Kim, H.-G. Chun, T.-Y. Cho, J.-S. Jung, and J.-G. Kang. Structural and Optical Properties of $BaMgAl_{10}O_{17}:Eu^{2+}$ Phosphor. *Chemistry of Materials*, 14(12):5045–5052, 2002.

R. D. Kirk. The Luminescence and Tenebrescence of Natural and Synthetic Sodalite. *American Mineralogist*, 40:22–31, 1955.

R. D. Kirk, J. H. Schulman, and H. B. Rosenstock. Structure in the luminescence emission of the $[S_2]^-$ Ion. *Solid State Communications*, 3(June):235–239, 1965.

A. Le Bail. Whole powder pattern decomposition methods and applications: A retrospection. *Powder Diffraction*, 20(4):316–326, 2005.

A. Mikuła, M. Król, and A. Koleżyński. Experimental and theoretical spectroscopic studies of Ag^-, Cd^- and Pb^-sodalite. *Journal of Molecular Structure*, 1126:110–116, 2016.

I. Norrbo, P. Gluchowski, I. Hyppänen, T. Laihinen, P. Laukkanen, J. Mäkelä, F. Mamedov, H. S. Santos, J. Sinkkonen, M. Tuomisto, A. Viinikanoja, and M. Lastusaari. Mechanisms of Tenebrescence and Persistent Luminescence in Synthetic Hackmanite $Na_8Al_6Si_6O_{24}(Cl,S)_2$. *ACS Applied Materials and Interfaces*, 8(18):11592–11602, 2016.

L. Pauling. The structure of sodalite and helvite. *Zeitschrift fuer Kristallographie, Kristallgeometrie, Kristallphysik, Kristallchemie*, 74:213 – 225, 1930.

N. Pradal, A. Potdevin, G. Chadeyron, and R. Mahiou. Structural, morphological and optical investigations on $BaMgAl_{10}O_{17}:Eu^{2+}$ elaborated by a microwave induced solution combustion synthesis. *Materials Research Bulletin*, 46(4):563–568, 2011.

H. M. Rietveld. A profile refinement method for nuclear and magnetic structures. *Journal of Applied Crystallography*, 2(2):65–71, June 1969.

H. Song, B. Chen, H. Peng, and J. Zhang. Light-induced change of charge transfer band in nanocrystalline $Y_2O_3:Eu^{3+}$. *Applied Physics Letters*, 81(10):1776–1778, aug 2002.

FMS The Fluorescent Mineral Society. Luminescence and Fluorescence, 2013. URL http://uvminerals.org/fms/luminescence.

Z. Wang, P. He, Y. Zhang, X. Li, L. Xiong, and J. Guo. Photoluminescence of $Y_2O_3:Eu^{3+}$ prepared by mimicking wood tissue. *Materials Letters*, 76:240–242, 2012.

T. Zahoransky, H. Friis, and M. A. W. Marks. Luminescence and tenebrescence of natural sodalites: a chemical and structural study. *Physics and Chemistry of Minerals*, 43(7):459–480, 2016.

Appendix

A Abbreviations and symbols

UV - Ultra-violet
IR - Infra-red
FTIR - Fourier Transform Infra-red
XRD - X-ray Diffraction
EDX - Energy Dispersive X-ray spectroscopy
OF650 - Sample with orange fluorescence synthesised at 650 °C
OBF650 - Sample with orange and blue fluorescence synthesised at 650 °C
BF600 - Sample with blue fluorescence synthesised at 600 °C
BF575 - Sample with blue fluorescence synthesised at 575 °C
NF575 - Sample with no fluorescence synthesised at 575 °C - chloride only, no sulfur

B Refinements

Le Bail Refinement

Le Bail refinement does not take atoms within a structure into account. Instead, it refines the fit of the calculated pattern based on structural properties, such as the lattice and profile parameters of the lattice. This is done by setting an arbitrary intensity value for all peaks in a calculated pattern, then altering the intensities and positions of peaks in this pattern, based on stepwise changes in these lattice and profile parameters, until the best fit to the observed data is obtained, [Le Bail, 2005].

Rietveld Refinement

Rietveld refinement extends Le Bail refinement, allowing analysis of an entire diffraction pattern, but becomes much more difficult for powders containing more than one phase. In addition to the lattice and profile parameters refined by Le Bail, Rietveld refinement can also refine atomic positions and occupancies, as well as displacements caused by heat in the system. Rietveld refinement was initially used for neutron diffraction data, as seen in [Rietveld, 1969].

Acknowledgements

My thanks to Prof. Chris Frost, as the head of department.

I would like to thank Prof. Mark Weller for providing the opportunity to perform this work.

I would also like to thank Dr Pascaline Patureau for sharing her work with me, for teaching me how to use all of the necessary equipment, and for providing me with the information and support that were needed to complete this project and write this report.

Finally, I would like to thank my parents for their support, for their corrections of my spelling and grammar, and for telling me where this report did not provide enough information to be understood.